metals

MDPI

Article

Mechanical Properties of High Strength Aluminum Alloy EN AW-7075 Additively Manufactured by Directed Energy Deposition

Anika Langebeck [1,*], Annika Bohlen [1], Rüdiger Rentsch [2] and Frank Vollertsen [1,3]

1 BIAS—Bremer Institut für angewandte Strahltechnik GmbH, Klagenfurter Str. 5, 28359 Bremen, Germany; bohlen@bias.de (A.B.); info-mbs@bias.de (F.V.)
2 Leibniz Institute for Material-Oriented Technologies, Badgasteiner Straße 3, 28359 Bremen, Germany; rentsch@lfm.uni-bremen.de
3 Faculty Production Technology, University of Bremen, Bibliothekstr. 1, 28359 Bremen, Germany
* Correspondence: langebeck@bias.de; Tel.: +49-421-218-58035

Received: 31 March 2020; Accepted: 23 April 2020; Published: 29 April 2020



Abstract: A manifold variety of additive manufacturing techniques has a significant positive impact on many industry sectors. Large components are often manufactured via directed energy deposition (DED) instead of using powder bed fusion processes (PBF). The advantages of the DED process are a high build-up rate with values up to 300 cm^3/h and a nearly limitless build-up volume. In combination with the lightweight material aluminum it is possible to manufacture large lightweight components with geometries adapted to customer requirements in small batches. This contributes the pursuit of higher efficiency of machines through lightweight materials as well as lightweight design. A low-defect additive manufacturing of high strength aluminum EN AW-7075 powder via DED is an important challenge. The laser power has a significant influence on the remaining porosity. By increasing the laser power from 2 kW to 4 kW the porosity in single welding tracks can be lowered from 2.1% to only (0.09 ± 0.07)% (n = 3). However, when manufacturing larger specimens; the remaining porosity is higher than in single tracks; which can be attributed to the oxide skin on the preceding welding tracks. Further investigations regarding the mechanical properties were carried out. In tensile tests an ultimate tensile strength of (222 ± 17) MPa (n = 6) was measured. The DED processed EN AW-7075 shows comparable mechanical properties to PBF processed EN AW-7075.

Keywords: directed energy deposition; EN AW-7075; porosity; ultimate tensile strength

1. Introduction

Metal additive manufacturing for producing components and component parts is becoming more and more relevant, especially in customized single and small series production [1]. Two relevant process groups are powder bed fusion (PBF) and directed energy deposition (DED) (ISO/ASTM 52900:2018-06). The latter is commercialized by several organizations and known under different acronyms such as LENS (Laser Engineering Net Shaping) [2]. These DED systems are used besides additive manufacturing purposes for repairing high-value components [3]. A common classification of DED processes is to divide them into powder-feed processes and wire-feed processes [4]. For PBF processes the powder material is supplied in a powder bed. For powder-feed DED, powder nozzles are used to deliver the powder directly into the process zone. In contrast to PBF processes, DED is used in case of larger structures with lower resolution [4] due to high build-up rates which can reach values up to 1.8 kg/h for the powder-feed DED and a nearly limitless build-up volume [5]. Besides a laser as energy source for DED an electron beam or an arc can be used. A five times higher build-up

rate can be achieved in DED with wire feed [6]. However, by using a laser as energy source the heat input is significantly lower compared to an arc and therefore the distortion is smaller [7].

When aluminum alloys are used in additive processes, hydrogen related porosity is a disadvantage that must be considered. Hydrogen related porosity is formed during solidification of the melt pool, when the solubility of the aluminum for hydrogen decreases significantly [8]. An important source for hydrogen besides the oxide layer on the substrate's surface is the humidity of the ambient air near to the process zone [9]. There are two approaches to reduce hydrogen related porosity. First, by improving the shielding gas coverage to protect the process zone from hydrogen. Secondly, by adapting the process parameters for a better degassing of hydrogen during the solidification of the melt pool.

A low porosity is necessary to achieve high mechanical characteristics such as ultimate tensile strength and Young's modulus. For additively manufactured tensile specimens made of aluminum EN AW-7075 laser powder bed fusion (LPBF) is often used [10]. Only few scientists report on produced tensile specimens using DED [11]. When additively manufactured tensile specimens are tested, it is shown that the orientation of the specimen's single tracks to the tensile load direction has a significant influence on the results for the mechanical characteristics. The ultimate tensile strength is highest when building direction is parallel to the load direction [11]. EN AW-7xxx alloys can be precipitation hardened in a subsequent heat treatment that results in higher hardness and therefore in higher ultimate tensile strength [12]. A T6 heat treatment is often used to achieve an increase in hardness through precipitation hardening [13]. Therefore, solution heat treatment followed by quenching is carried out to achieve a supersaturated solid solution. Precipitation of magnesium and zinc take place during subsequent artificial aging and an increase in hardness is reached. For DED manufactured specimens of an EN AW-7xxx alloy with high zinc content of 11.9% and high magnesium content of 2.7% the measured Vickers hardness increased after a T6 heat treatment from (133 ± 6) HV0.05 to (219 ± 4) HV0.05 [13]. When processing EN AW-7xxx alloys in DED processes a loss in volatile elements such as zinc and magnesium is observed [14]. This alters the initial alloy composition and can affect the (mechanical) properties.

In this study low-defect specimens of EN AW-7075 will be manufactured via powder-feed DED with an adapted shielding gas shroud and the influence of the laser power on the porosity will be determined. The low-defect specimens will be used to examine the influence of artificial aging on hardness and mechanical characteristics of the low-defect specimens will be evaluated as well.

2. Materials and Methods

The specimens were manufactured by powder-feed DED. Therefore, a lamp pumped Nd:YAG rod laser (Trumpf GmbH + Co. KG, Ditzingen, Germany) was used. The Trumpf HL 4006 D generates a wavelength of 1064 nm with a maximum power of 4 kW. The laser beam is guided via an optical fiber with a core diameter of 600 µm to the processing head. The processing head consists out of an optical unit by Trumpf (type BEO D70). Collimation lens as well as focus lens have a focal length of 200 mm. By setting the laser focus with a top-hat profile 24.5 mm above the substrate surface a calculated spot size of 4.5 mm with a gaussian intensity distribution on the substrate's surface was reached. With increasing the laser power to the maximum of 4 kW at a spot size of 4.5 mm a maximum laser intensity of 251 W/cm^2 can be reached. This ensures that the threshold intensity for forming a keyhole is not exceeded during the DED process. The aluminum powder was supplied by a rotating disk powder feeder made by Plasma-Technik AG (Twin10C, Wohlen, The Switzerland) to a coaxial three-jet nozzle by Ixun Lasertechnik GmbH (Aachen, Germany) with a working distance for the powder focus of 12 mm. Argon was used as carrier and shielding gas. Substrates for the specimens and the processing head were mounted on a 3-axis CNC by Föhrenbach GmbH (Löffingen-Unadingen, Germany) and which was driven by a control unit from Power Automation GmbH (type PA8000, Pleidelsheim, Germany).

As substrate material aluminum wrought alloys EN AW-5083 and EN AW-6082 with a thickness of 10 mm each were used. The used aluminum powder EN AW-7075 was supplied by NMD—New Materials Development GmbH (Heemsen, Germany) with a grain size distribution of D_{10} 37 µm, D_{50} 68 µm and D_{90} 122 µm. It was sieved with 50 µm and 125 µm mesh size. See Table 1 for the chemical composition of the powder material.

Table 1. Chemical composition of EN AW-7075 in wt. % supplied by NMD—New Materials Development GmbH (Heemsen, Germany). Measurements in accordance with EN 10204 3.1.

Al	Si	Fe	Mn	Zn	Mg	Cu	Cr
89.9	0.11	0.09	0.01	5.51	2.42	1.60	0.21

In order to improve the shielding gas coverage of the processing zone an additional shielding gas shroud was developed. See Figure 1 for a schematic view of the developed shielding gas shroud. The shroud is made of sinter metal with an internal radius of 19 mm and an external radius of 47 mm and has four ports for the gas supply to provide an extended and homogenous shielding gas coverage for the process zone.

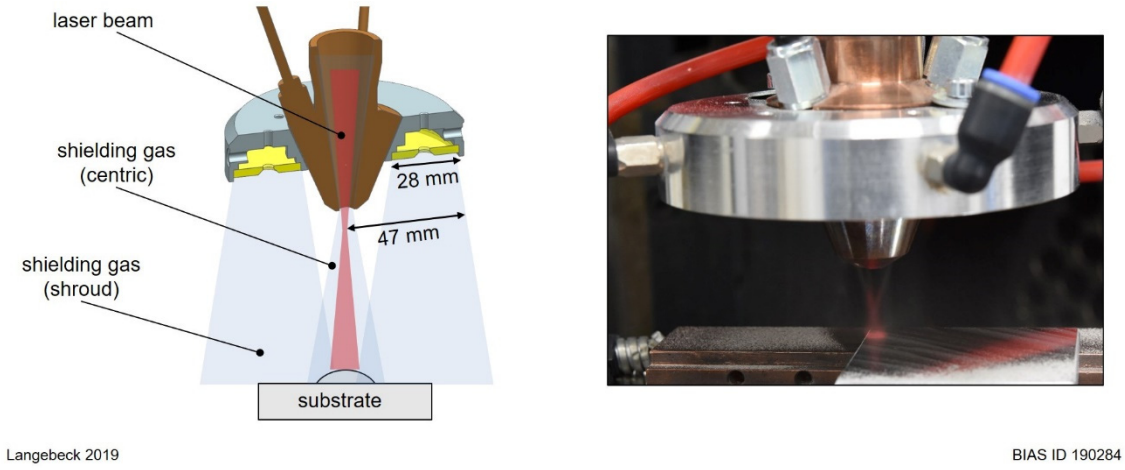


Figure 1. Improved shielding gas concept with an additional shielding gas shroud.

The effect of the new shielding gas concept was evaluated by manufacturing single tracks (see Table 2). The porosity was measured at cross sections. A decrease in porosity from over 7.0% to 5.9% was measured. This corresponds to a reduction by 1/8 for the used parameter set. For all subsequent experimental studies regarding DED with EN AW-7075 the additional shielding gas shroud was used.

The influence of the laser power on pore volume was determined at cross sections in the area of the center of the specimens. The laser power was varied between 2 kW and 4 kW in steps of 0.5 kW. Each parameter combination was examined in randomized triple determination.

For measuring the tensile strength as well as the hardness of the additively manufactured aluminum parts larger specimens consisting of 9 layers in total with 6 single tracks per layer were manufactured. A horizontal overlapping (y-direction) between the single layers of 30% was used. The vertical overlapping (z-direction) was 13%. Between two subsequent layers an offset in y-direction of 2.5 mm was chosen. The building direction (x-direction) was parallel to the load direction chosen for the tensile tests. For the evaluation of the porosity, the microscopic images of non-etched cross-sections were binarized using Otsu's method. See Figure 2 for the position of the cross-sections. The binarized images were used to calculate the porosity by measuring the proportion of black (pores) to white pixels (EN AW-7075). The Vickers hardness measurements were carried out on ground and polished cross sections directly after the DED process and after artificial aging according DIN EN ISO 6507-3. By using wire-cut EDM (electrical discharge machining) tensile specimens were manufactured out of

the artificially aged DED parts with an overall length of 100 mm, a width of grip section of 25 mm, a width of 10 mm and a thickness of 4 mm (see Figure 2). The artificial aging includes stretching to 2% elongation, aging for 3 days at room temperature and two step artificial aging for 18 h at 120 °C and for 5 h at 175 °C.

Table 2. Process parameters for single tracks to determine the influence of shielding gas concept on pore volume and the influence of energy input per unit length on pore volume.

Parameters	Single Tracks for Shielding Gas Investigations	Single Tracks for Porosity Investigations
Laser power	2.4 kW	2 kW to 4 kW
Laser spot diameter	2.0 mm	4.5 mm
Shielding gas flow conv.	7.5 L/min (centric)	-
Shielding gas flow with additional shroud	7.5 L/min (centric)	7.5 L/min (centric)
	30 L/min (additional shroud)	30 L/min (additional shroud)
Carrier gas flow	5.5 L/min	4 L/min
Powder feed rate	(9.9 ± 0.2) g/min	(9.3 ± 0.3) g/min
Substrate material	EN AW-5083	EN AW-5083
Welding speed	400 mm/min	400 mm/min

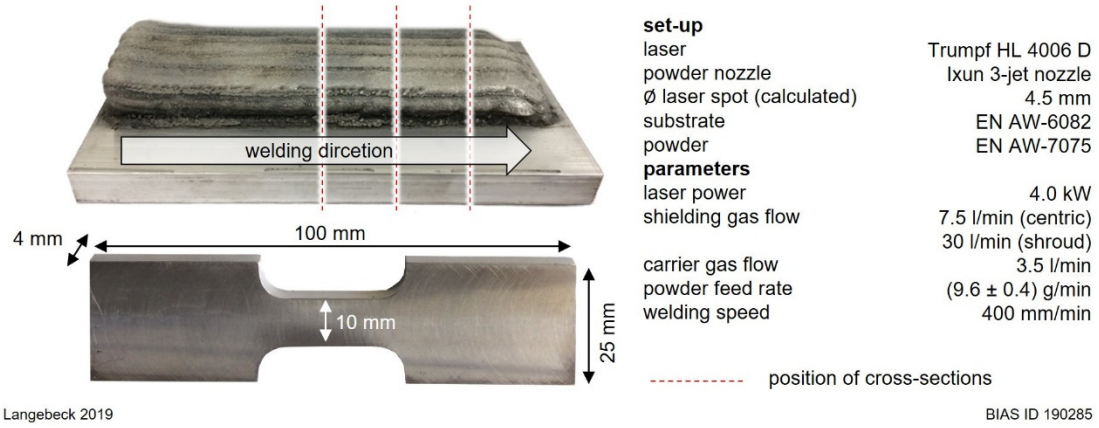


Figure 2. Additively manufactured tensile specimen with building direction parallel to load direction before and after wire-cut electrical discharge machining (EDM).

3. Results

As shown in Figure 3 with increased laser power from 2 kW to 4 kW the measured porosity decreased from 2.1% to just (0.09 ± 0.07)% (n = 3). With a powder feed rate of (9.3 ± 0.3) g/min and a powder usage efficiency of (82.0 ± 3.4)% (n = 14) a build-up rate of (164 ± 10) cm^3/h (n = 14) was reached.

When manufacturing larger parts consisting of several layers with several single tracks the low pore volume of (0.09 ± 0.07)% (n = 3) measured in single tracks could not be reached anymore. However, a pore volume of (2.2 ± 0.9)% (n = 15) was reached. Figure 4 shows an exemplary cross section. The cross section reveals a preferred localization of the pores in the area of the melt pool borders. Additionally to porosity some cracks between the lower layers and the substrate material on the left and right side are visible.

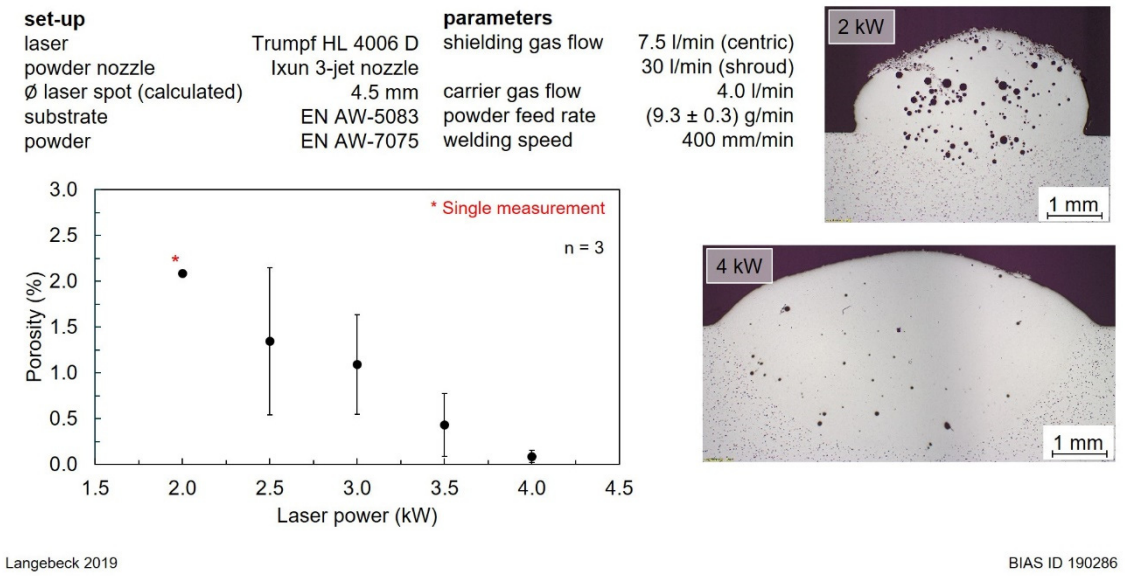


Figure 3. Influence of laser power on porosity.

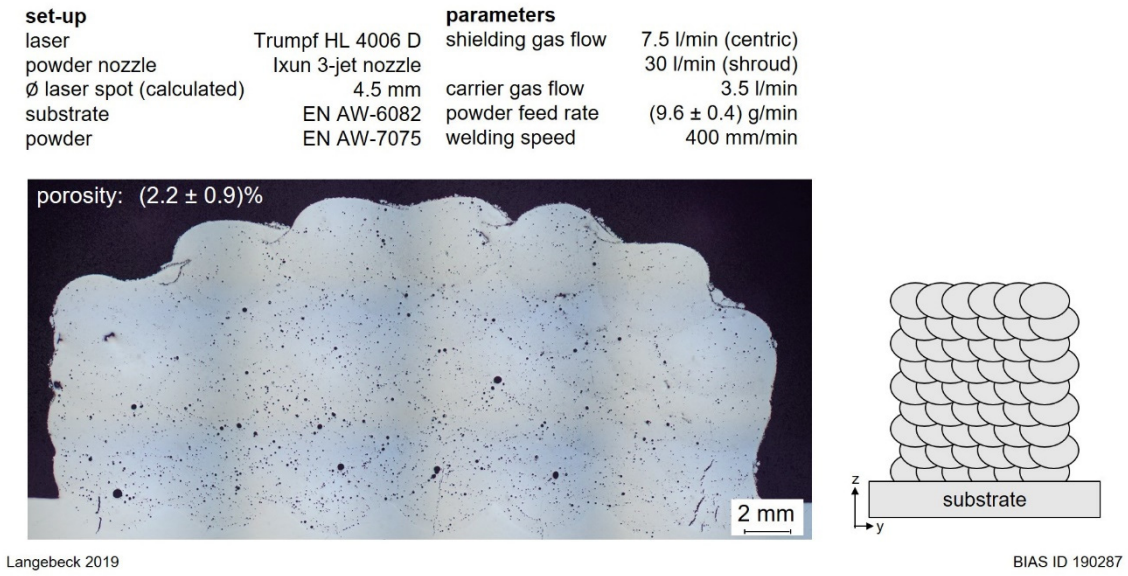


Figure 4. Schematic view of built-up strategy; cross section of large part for hardness measurements as well as tensile tests.

After the DED process Vickers hardness measurements were carried out. A hardness of (85 ± 4) HV0.5 (n = 4) was measured. A slight improvement in hardness up to (93 ± 2) HV0.5 (n = 3) could be reached after artificial aging.

After artificial aging tensile specimens were manufactured and tested. The results are shown in Figure 5. An ultimate tensile strength of (222 ± 17) MPa (n = 6) was calculated.

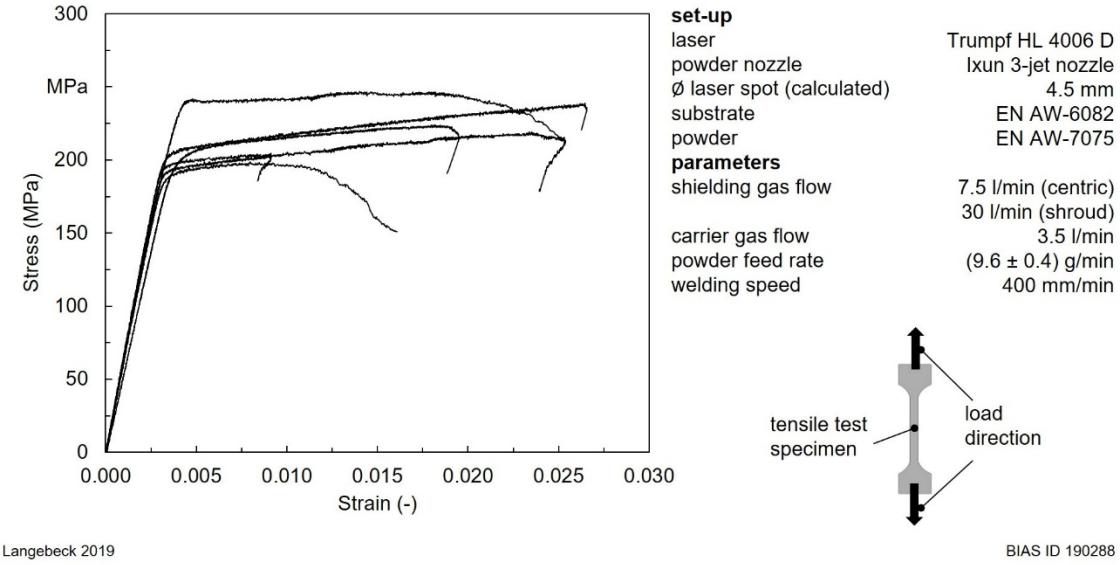


Figure 5. Results of tensile tests for additively manufactured specimens made of EN AW-7075.

4. Discussion

In this work, low-defect specimens were manufactured via DED with an additional shielding gas shroud. An increase in laser power leads to a significant decrease in porosity. This parameter set were then used to evaluate the mechanical characteristics of (tensile) specimens made of EN AW-7075.

The pore volume of DED processed EN AW 7075 decreased from 2.09% to just (0.09 ± 0.07)% (n = 3) in single track experiment by the increase of laser power from 2 kW to 4 kW. The increased laser power led to a more overheated and larger melt pool. Additionally, the thermo-capillary convection in the melt pool increases with higher laser power [15]. This aspect results in lower cooling rates which leave the precipitated gaseous hydrogen and other volatile elements such as zinc and magnesium from the alloy system longer time for degassing out. When larger specimens are manufactured with the same parameter set, which was used for single tracks, the low pore volume of single track experiment could not be achieved. A reason for this can be hydrated oxide layers which form on the substrate surfaces as well as on previous weld beads [16]. The weld beads have a convex macroscopic geometry and have a rough surface due to adhering, partially melted powder particles. This significantly increases the surface area that can oxidize and hydrate. In addition, the increased temperatures during the welding of the individual layers further increase the thickness of the resulting oxide layer [17]. The surface of the weld beads can be identified as a significant source for additional hydrogen that causes porosity. The previous welding tracks are partially remelted during the DED process and the oxide layer with its hydrogen content can cause porosity in the area of the melt pool borders of the new welding track.

EN AW-7075 can be precipitation hardened. Highest hardness can be reached after a T6 heat treatment. The large specimens for hardness measurements were artificially aged without a previous solution heat treatment. The results show a slight increase in hardness from (85 ± 4) HV0.5 (n = 4) to (93 ± 2) HV0.5 (n = 3). This indicates that after the DED process a microstructure is already present which achieves precipitation hardening by artificial aging. For conventionally produced EN AW-7075 T6 a Vickers hardness of (177 ± 7) HV0.5 (n = 3) was measured, which is considerably higher. It is uncertain whether a higher increase in hardness can be achieved by previous solution heat treatment with quenching and subsequent artificial aging reaching a T6 condition. The measured ultimate tensile strength of (222 ± 17) MPa (n = 6) and elongation of about 2% for the DED specimens are in good agreement with the mechanical characteristics of specimens additively manufactured by LPBF (laser powder bed fusion) with an ultimate tensile strength of (206 ± 26) MPa and an elongation smaller than 1% [10]. These comparative figures were determined for both as-built specimens and solution annealed, quenched and artificially aged specimens with no significant deviations [10]. This suggests

that a complete T6 heat treatment after the DED process would have had a similar negligible effect on the ultimate tensile strength as for the LPBF specimens. Though when comparing the measured ultimate tensile strength of (222 ± 17) MPa (n = 6) with the tensile strength of conventionally produced EN AW-7075 for T6 temper with 572 MPa, it becomes apparent that the additively manufactured specimen's tensile strength is considerably lower yet it shows good agreement with the tensile strength of soft annealed aluminum with 228 MPa [18]. However, the elongation of only 2% for the additively manufactured specimens is uncharacteristic for the aluminum alloy EN AW-7075 which normally has an elongation of 11% to 17% [18]. This leads to the assumption that the additively manufactured specimens could reach higher ultimate tensile strength if the elongation could be enlarged. The loss in elongation can be attributed to the defects within the specimens such as porosity and hot cracks (see Figure 4) and therefore further improvement for low-defect DED is crucial.

5. Conclusions

Low-defect aluminum specimens can be manufactured via DED by increasing the time for degassing through an increase in laser power. Whereby the surface of the previous welding tracks has a significant impact on porosity, too. After the DED process the EN AW-7075 specimens have a microstructure which allows for a slight increase in hardness from (85 ± 4) HV0.5 (n = 4) to (93 ± 2) HV0.5 (n = 3) through precipitation hardening. The mechanical characteristics do not reach those of conventionally produced EN AW-7075 T6 specimens, which is mostly attributable to the remaining defects. When comparing the measured ultimate tensile strength of (222 ± 17) MPa (n = 6) with that of other additively manufactured EN AW-7075 specimens, good agreement is obtained irrespective of whether the specimens were heat treated or not.

Author Contributions: Conceptualization, A.L., A.B. and R.R.; data curation, A.L.; formal analysis, A.L. and R.R.; investigation, A.L. and R.R.; methodology, A.L. and R.R.; project administration, A.B.; resources, F.V.; supervision, A.B. and F.V.; validation, A.L., A.B., R.R. and F.V.; visualization, A.L.; writing—original draft, A.L.; writing—review & editing, A.B. and F.V. All authors have read and agreed to the published version of the manuscript.

Funding: This research was funded by the Federal Ministry for Economic Affairs and Energy (BMWi) via the German Federation of Industrial Research Associations (AiF) in accordance with the policy to support the Central Innovations of Medium-Sized Enterprises (ZIM) on the basis of a decision by the German Bundestag, grant number ZF4063003SU7.

Acknowledgments: The authors gratefully acknowledge the collaboration with the company IBO GmbH regarding their support of knowledge over the course of the research. The "BIAS ID" numbers are part of the figures and allow the retraceability of the results with respect to the mandatory documentation required by the funding organization.

Conflicts of Interest: The authors declare no conflict of interest.

References

1. Schmidt, M.; Merklein, M.; Bourell, D.; Dimitrov, D.; Hausotte, T.; Wegener, K.; Overmeyer, L.; Vollertsen, F.; Levy, G.N. Laser based additive manufacturing in industry and academia. *CIRP Ann.* **2017**, *66*, 561–583. [CrossRef]
2. Saboori, A.; Gallo, D.; Biamino, S.; Fino, P.; Lombardi, M. An overview of additive manufacturing of titanium components by directed energy deposition: Microstructure and mechanical properties. *Appl. Sci.* **2017**, *7*, 883. [CrossRef]
3. Saboori, A.; Aversa, A.; Marchese, G.; Biamino, S.; Lombardi, M.; Fino, P. Application of directed energy deposition-based additive manufacturing in repair. *Appl. Sci.* **2019**, *9*, 3316. [CrossRef]
4. Jahn, S.; Matthes, S.; Scheller, D.; Huber, M. Process principles for metal additive manufacturing. In Proceedings of the IIW Commissions I, IV, XII, SG 212 Joint Intermediate Meeting, Greifswald, Germany, 7–12 July 2019.
5. Ding, D.; Pan, Z.; Cuiuri, D.; Li, H. Wire-feed additive manufacturing of metal components: Technologies, developments and future interests. *Int. J. Adv. Manuf. Technol.* **2015**, *81*, 465–481. [CrossRef]
6. Wohlers, T. *Wohlers Report 2014: 3D Printing and Additive Manufacturing State of the Industry Annual Worldwide Progress Report*; Wohlers Associates: Fort Collins Col, CO, USA, 2014.

7. Ding, J.; Colegrove, P.; Mehnen, J.; Ganguly, S.; Sequeira Almeida, P.M.; Wang, F.; Williams, S. Thermo-mechanical analysis of Wire and Arc Additive Layer Manufacturing process on large multi-layer parts. *Comput. Mater. Sci.* **2011**, *50*, 3315–3322. [CrossRef]
8. Zhao, H.; White, D.R.; DebRoy, T. Current issues and problems in laser welding of automotive aluminium alloys. *Int. Mater. Rev.* **1999**, *44*, 238–266. [CrossRef]
9. Guo, G.; Zhang, M.; Chen, H.; Chen, J.; Li, P.; Yang, Y.P. Effect of humidity on porosity, microstructure and fatigue strength of A7N01S-T5 aluminum alloy welded joints in high-speed trains. *Mater. Des.* **2015**, *85*, 309–317.
10. Reschetnik, W.; Brüggemann, J.-P.; Aydinöz, M.E.; Grydin, O.; Hoyer, K.-P.; Kullmer, G.; Richard, H.A. Fatigue crack growth behavior and mechanical properties of additively processed EN AW-7075 aluminium alloy. *Procedia Struct. Integr.* **2016**, *2*, 3040–3048. [CrossRef]
11. Khazan, P.; Stroth, M.; Freiße, H.; Köhler, H. Mechanical Properties of Large Three-Dimensional Specimens Build through Direct Powder Deposition. *WGP Congr.* **2014**, *1018*, 525–532. [CrossRef]
12. Brüggemann, J.-P.; Risse, L.; Kullmer, G.; Richard, H.A. Optimization of the fracture mechanical properties of additively manufactured EN AW-7075. *Procedia Struct. Integr.* **2018**, *13*, 311–316. [CrossRef]
13. Wang, P.; Li, H.C.; Prashanth, K.G.; Eckert, J.; Scudino, S. Selective laser melting of Al-Zn-Mg-Cu: Heat treatment, microstructure and mechanical properties. *J. Alloys Compd.* **2017**, *707*, 287–290. [CrossRef]
14. Singh, A.; Ramakrishnan, A.; Dinda, G. Direct laser metal deposition of Al 7050 alloy. *SAE Tech. Paper* **2017**. [CrossRef]
15. Dai, D.; Gu, D. Influence of thermodynamics within molten pool on migration and distribution state of reinforcement during selective laser melting of AlN/AlSi10Mg composites. *Int. J. Mach. Tools Manuf.* **2016**, *100*, 14–24. [CrossRef]
16. Haboudou, A.; Peyre, P.; Vannes, A.B.; Peix, G. Reduction of porosity content generated during Nd:YAG laser welding of A356 and AA5083 aluminium alloys. *Mater. Sci. Eng. A* **2003**, *363*, 40–52. [CrossRef]
17. Jeurgens, L.P.H.; Sloof, W.G.; Tichelaar, F.D.; Mittemeijer, E.J. Growth kinetics and mechanisms of aluminum-oxide films formed by thermal oxidation of aluminum. *J. Appl. Phys.* **2002**, *92*, 1649–1656. [CrossRef]
18. Davis, J.R. *Properties and Selection*, 10th ed.; ASM International: Materials Park, OH, USA, 2000.



© 2020 by the authors. Licensee MDPI, Basel, Switzerland. This article is an open access article distributed under the terms and conditions of the Creative Commons Attribution (CC BY) license (http://creativecommons.org/licenses/by/4.0/).